Constraining the Properties of the Eta Carinae System via 3-D SPH Models of Space-Based Observations: The Absolute Orientation of the Binary Orbit

Thomas I. Madura[1], Theodore R. Gull[2], Stanley P. Owocki[1], Atsuo T. Okazaki[3], and Christopher M.P. Russell[1]

[1] University of Delaware, Newark, DE, USA
[2] NASA Goddard Space Flight Center, Greenbelt, MD, USA
[3] Hokkai-Gakuen University, Sapporo, Japan

Abstract: The extremely massive (> 90 $M_\odot$) and luminous ($= 5 \times 10^6$ $L_\odot$) star Eta Carinae, with its spectacular bipolar "Homunculus" nebula, comprises one of the most remarkable and intensely observed stellar systems in the galaxy. However, many of its underlying physical parameters remain a mystery. Multiwavelength variations observed to occur every 5.54 years are interpreted as being due to the collision of a massive wind from the primary star with the fast, less dense wind of a hot companion star in a highly elliptical ($e \sim 0.9$) orbit. Using three-dimensional (3-D) Smoothed Particle Hydrodynamics (SPH) simulations of the binary wind-wind collision in Eta Car, together with radiative transfer codes, we compute synthetic spectral images of [Fe III] emission line structures and compare them to existing *Hubble Space Telescope*/Space Telescope Imaging Spectrograph (*HST*/STIS) observations. We are thus able, for the first time, to constrain the absolute orientation of the binary orbit on the sky. An orbit with an inclination of $i \sim 40°$, an argument of periapsis $\omega \sim 255°$, and a projected orbital axis with a position angle of $\sim 312°$ east of north provides the best fit to the observations, implying that the orbital axis is closely aligned in 3-D space with the Homunculus symmetry axis, and that the companion star orbits clockwise on the sky relative to the primary.

1 Introduction

The direct detection of the hot companion star Eta Car B has proven to be quite difficult, especially since at UV, Visible, and IR wavelengths the extended wind of the primary star Eta Car A dominates the spectrum. Given the lack of direct signatures of Eta Car B, the focus has recently shifted to examining spectral features formed in the wind-wind collision region and circumstellar ejecta near Eta Car A (Verner et al. 2005; Nielsen et al. 2007; Mehner et al. 2010). In a further attempt to spatially characterize the wind-wind interaction region, Gull et al. (2009) presented an analysis of *HST*/STIS observations obtained between 1998 and 2004, identifying spatially extended, velocity-resolved forbidden emission lines from low- (IP $<$ 13.6 eV) and high- (IP $>$ 13.6 eV) ionization species. More importantly, Gull et al. (2009) show how proper modeling of the *HST*/STIS slit spectra, which provide valuable spatial *and* velocity information, has the potential to constrain the absolute orientation and direction of the binary orbit on the sky by removing the ambiguity inherent to models based solely

on the observed RXTE X-ray light curve or other point-source data. As an extension of the work in Gull et al. (2009), we present a 3-D dynamical model for the high-ionization forbidden line emission observed in Eta Car with *HST*/STIS. This model is based on the results of 3-D SPH simulations of the colliding winds and radiative transfer calculations performed with a modified version of the SPLASH (Price 2007) code. Synthetic spectro-images are generated from the models and compared to the observations with the goal of constraining the absolute orientation and direction of the binary orbit.

2 Observations

Observations of high- and low-ionization forbidden emission lines were obtained from March 1998 to March 2004 with the *HST*/STIS (0.1″ angular resolution, $R \sim 8000$), and are described in detail in Gull et al. (2009). Figure 1 presents example spectro-images of resolved, broad forbidden lines of both high and low ionization. The leftmost panel is an *HST*/ACS HRC image of the central 2″ of Eta Car with a 2″ × 0.1″ portion of the STIS aperture shown at position angle (PA) = +38°. The three black dots correspond to Weigelt blobs B, C, and D, while the direction of north is shown in the top left corner. For an adopted distance of 2.3 kpc to Eta Car, 0.1″ = 230 AU. The middle two panels of Figure 1 are spectro-images of [Fe III] and [N II] (IP's = 16.2 & 14.5 eV) recorded May 5, 2003 (orbital phase $\phi = 0.976$) at this same STIS PA. In both cases the emission structures appear as well-defined blue-shifted rings that extend spatially up to $\sim 0.35''$ from the central source. For comparison, a spectral image of [Fe II] (IP = 7.9 eV) is presented in the rightmost panel. Notice the much more extended, red- and blue-shifted double-ring emission structures. As noted in Gull et al. (2009), the observed emission structures change with both orbital phase and STIS PA (see Figure 2), providing further insights into the geometry and physics of Eta Car's extended wind structure.

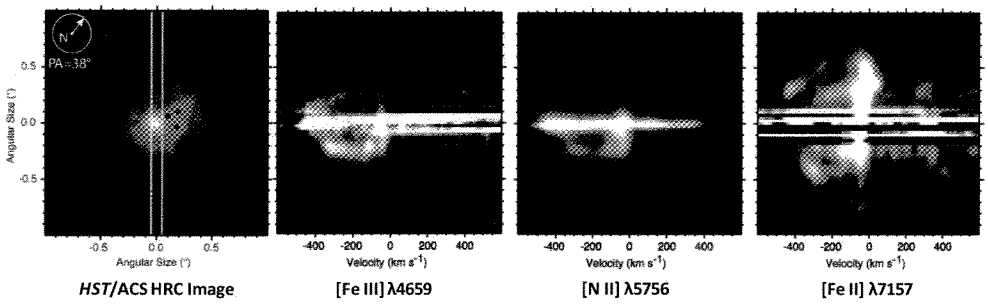

Figure 1: ***Leftmost panel***: *HST*/ACS HRC image of the central 2″ of Eta Car with the 0.1″ wide STIS aperture at PA = +38°. ***Middle 2 panels***: Spectro-images of the high-ionization lines of [Fe III] and [N II] (IP's = 16.2 & 14.5 eV) recorded at orbital phase $\phi = 0.976$. ***Rightmost panel***: Spectro-image of the low-ionization line of [Fe II] (IP = 7.9 eV), taken at the same phase and STIS PA (+38°).

3 A 3-D Dynamical Model for the Forbidden Line Emission

The 3-D dynamical model for the high-ionization, forbidden line emission is based on the results from 3-D SPH simulations of the binary colliding winds in the Eta Car system. SPH model parameters are similar to those of Okazaki et al. (2008), except that the new simulations assume a factor of four higher mass-loss rate for the primary star (10^{-3} $M_\odot$/yr), use adiabatic cooling, and have a 10× larger computational domain (corresponding to a box size of $\sim \pm 1550$ AU). For a desired orbital phase, the volume of material ionized by Eta Car B, assuming that it is an O5 giant with $10^{49.48}$ H ionizing photons/second (Mehner et al. 2010; Martins, Schaerer, & Hillier 2005), is found, followed by a

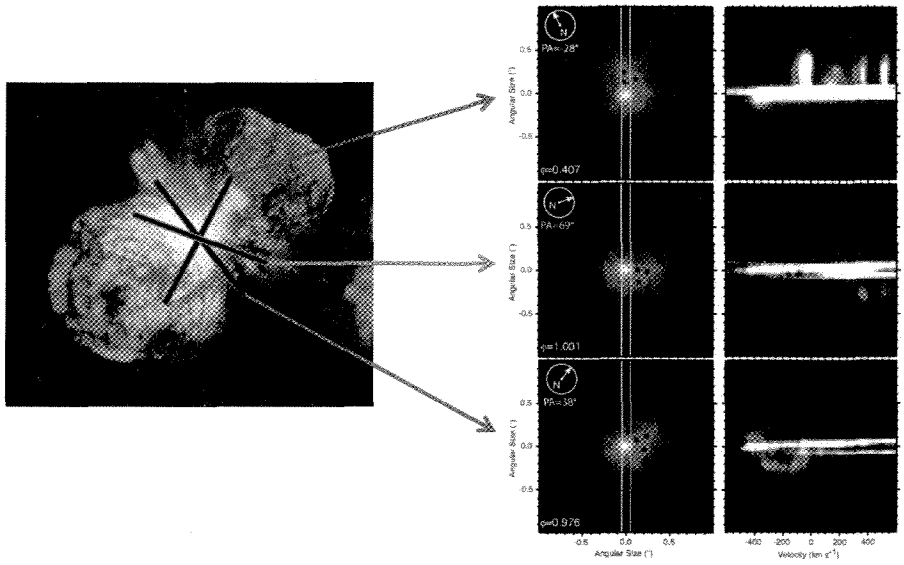

Figure 2: ***Left***: *HST*/WFPC2 image of Eta Car with the STIS aperture shown at PAs of $-28°$ (red), $+69°$ (green), and $+38°$ (blue). ***Right***: Corresponding ACS HRC image (left column) and observed spectro-image (right column, from top down) at phases $\phi = 0.407$, 1.001, and 0.976.

computation of the emissivity in the [Fe III] 4659Å line (IP = 16.2 eV) assuming a 2-level atom and collisional ionization equilibrium. A synthetic spectral image is made by orienting the 3-D binary wind structure on the sky at a specific PA and sampling the [Fe III] emissivity in the spatial/velocity plane of the *HST*/STIS long slit. The synthetic spectro-images are then convolved with a Gaussian ($0.1''$ and $\lambda/\Delta\lambda = 8000$) to better match the spatial and spectral resolutions of *HST*/STIS. For details on the modeling, see Madura (2010).

4 Results

The blue-shifted, ring-like emission feature shown in the middle panels of Figure 1 was modeled first since it represents a well-defined structure observed at a specific orbital phase and STIS PA. A parameter study was performed where the orbital inclination i, argument of periapsis ω, and position angle of the projected (on the sky) orbital axis of the system were varied in $10°$, $15°$, and $10°$ increments, respectively. Figure 3 helps illustrate the main results of this parameter study, assuming $i = 45°$ and an orbital axis at the same PA on the sky as the Homunculus symmetry axis ($312°$), at four values of the argument of periapsis $\omega = 0°$, $90°$, $180°$, and $270°$. It was found that only orbital orientations with values of ω near $270°$ are able to reproduce the observations, regardless of the assumed value of i or position angle of the projected orbital axis. Moreover, only orientations with $i \sim 40° - 60°$ and a projected orbital axis that is closely aligned with the Homunculus symmetry axis yield results that closely match the observed ring-like emission structure in both velocity and spatial extent.

The orbital orientation was further constrained by modeling a variety of observations obtained at different STIS PAs and orbital phases. In order to simultaneously reproduce the observed blue-shifted, ring-like emission feature at phase 0.976 and STIS PA = $+38°$, and the temporal variations in emission seen at other phases and STIS PAs, the binary system needs to have $i \approx 40° \pm 10°$, $\omega \approx 255° \pm 15°$, and an orbital axis projected on the sky with a PA $\approx 312° \pm 15°$ (Figure 4). This implies that the orbital axis is closely aligned in three-dimensional space with the symmetry axis of the Homunculus, with the resulting projected orbit on the sky having Eta Car B moving clockwise relative to Eta Car A, and apastron on the observer's side of the system (Figure 5).

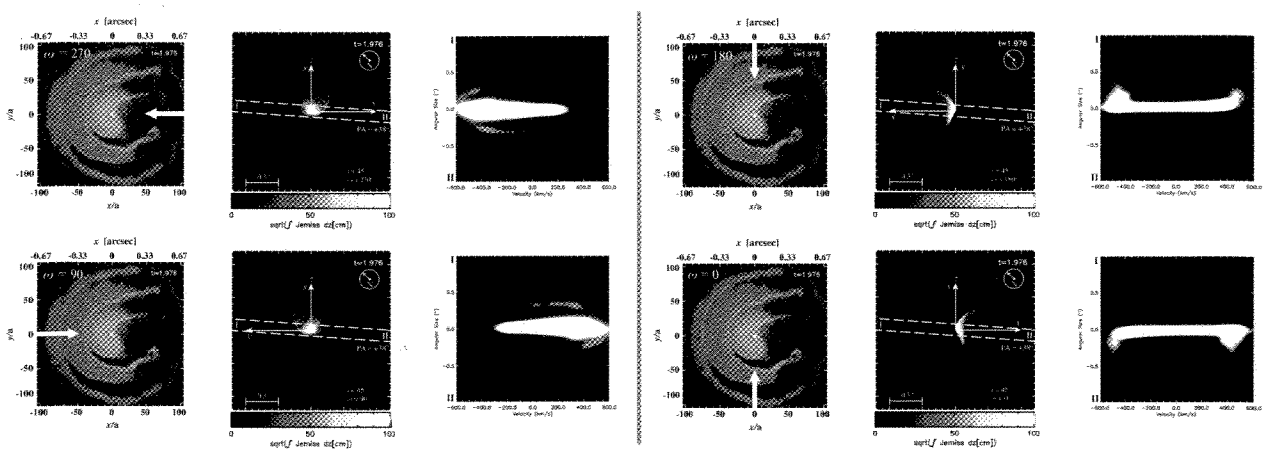

Figure 3: Illustration showing how the synthetic spectro-images depend on the orientation of the binary orbit. Each set of three images corresponds to a different value of ω. ***Left*****:** $\omega = 270°$ (top) and $90°$ (bottom). ***Right*****:** $\omega = 180°$ (top) and $0°$ (bottom). The 1st and 4th columns show slices of log density in the orbital plane from the 3-D SPH simulation at phase 1.976. The white arrow indicates the direction of the observer's line-of-sight. The 2nd and 5th columns show the 2-D projection on the sky of the square root of the intensity in the [Fe III] λ4659 line, assuming $i = 45°$ and a projected orbital axis that is aligned with the Homunculus symmetry axis. The projected semi-major (x), semi-minor (y), and orbital (z) axes are shown, as is the direction of north. Overlaid is the $0.1''$ wide STIS aperture at PA $= +38°$. Roman numerals I and II indicate the tops and bottoms of the slits, respectively. The 3rd and 6th columns show the corresponding synthetic slit spectro-images.

5 Conclusions

The 3-D dynamical model and observations constrain, for the first time, the absolute orientation of the binary orbit, implying an orbital axis that is closely aligned in 3-D space with the Homunculus symmetry axis, and a companion star that orbits clockwise on the sky. The observations are best fit assuming an inclination $i \approx 40°$, argument of periapsis $\omega \approx 255°$, and a projected orbital axis with a position angle on the sky of $\sim 312°$. The modeling shows that most of the high-ionization forbidden line emission originates in the inner $\pm 0.1''$ of the system and is due to the unresolved current-day wind-wind interaction region excited by the far-UV of the hot companion star Eta Car B. The blue-shifted, spatially extended ring-like emission structures observed at phase 0.976 and STIS PA $= +38°$ originate in the dense, compressed shells of the outflowing wind-wind interaction region created during the previous orbital cycle. Spectral variations in emission with orbital phase are due to orbital motion of Eta Car B, which causes different portions of the extended wind structures to be ionized. The disappearance of the high-ionization forbidden emission during periastron is attributed to the wrapping of the dense primary wind around the binary system, trapping the far-UV radiation from Eta Car B. Finally, observed variations in the emitting structures with STIS PA are due to the narrow STIS aperture sampling different specific regions of the projected wind structures.

The predicted alignment of the orbital and Homunculus axes, if confirmed, could have important implications for theories governing the formation of the Homunculus and/or the present shape of Eta Car A's wind. Binarity may turn out to have played an important role in the Great Eruption of the 1840s, and possibly the smaller eruption that later formed the Little Homunculus. If the orbital axis and rotation axis of Eta Car A are also aligned, this could provide support for theories of the Homunculus' formation that are based on radiation-driven mass loss from a rapidly rotating primary star. Further modeling and observations will help test the above conclusions.

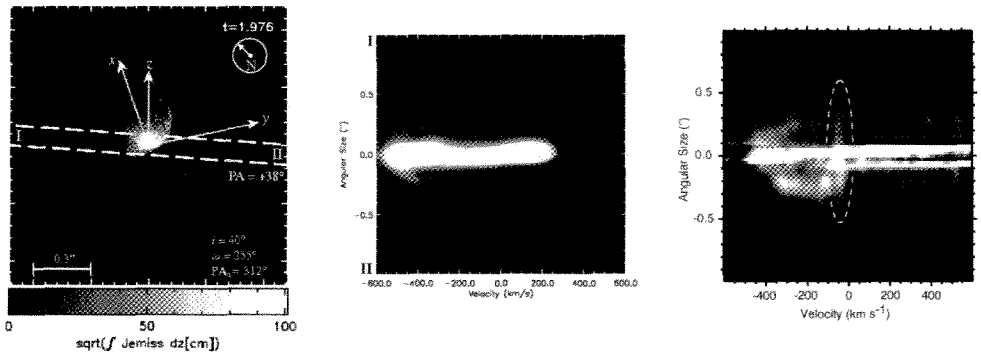

Figure 4: Best-fit model for matching the ring-like emission feature at phase 0.976 and STIS PA = $+38°$. ***Left***: 2-D projection of the square root of the intensity of the [Fe III] line for $i = 40°, \omega = 255°$, and a projected orbital axis aligned with the Homunculus symmetry axis. Overlaid is the $0.1''$ wide STIS slit. ***Middle***: Resulting synthetic spectro-image. ***Right***: Observed spectro-image. The emission feature circled in white originates in the dense, slow-moving Weigelt blobs and should be ignored.

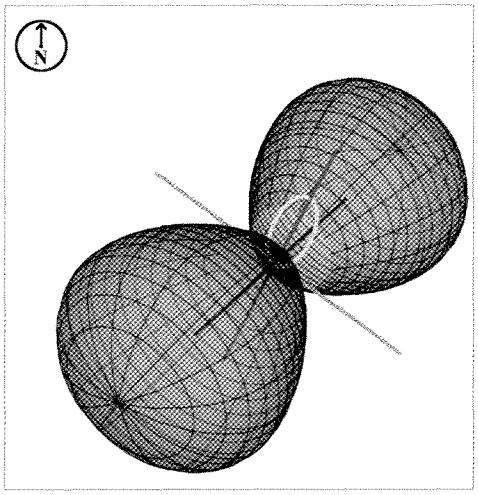

Figure 5: Illustration of the derived binary orbit (yellow) relative to the Homunculus (not to scale), projected on the sky, for $i = 40°$, $\omega = 255°$, and an orbital axis (blue) that is aligned with the Homunculus polar axis. The projected semi-major (red) and semi-minor (green) axes are also shown.

Acknowledgements

Observations were accomplished using *HST*/STIS observations from programs 9420, 9973, 11506, and archival research under 11273 and 10955. This work was funded by a NASA GSRP Fellowship.

References

Gull, T.R., Nielsen, K.E., Corcoran, M.F., et al., 2009, MNRAS, 396, 1308
Madura, T.I., 2010, Ph.D. Dissertation, University of Delaware
Martins, F., Schaerer, D., and Hillier, D. J., 2005, A&A, 436, 1049
Mehner, A., Davidson, K., Ferland, G.J., and Humphreys, R.M., 2010, ApJ, 710, 729
Nielsen, K.E., Corcoran, M.F., Gull, T.R., et al., 2007, ApJ, 660, 669
Okazaki, A.T., Owocki, S.P., Russell, C.M.P., and Corcoran, M.F., 2008, MNRAS, 388, L39
Price, D.J., 2007, Publications of the Astronomical Society of Australia, 24, 159
Verner, E., Bruhweiler, F., and Gull, T., 2005, ApJ, 624, 973